New Polyketides from Embellisia eureka, an endophyte of Cladanthus arabicus

Journal:	*Chirality*
Manuscript ID:	CHIR-12-0116
Wiley - Manuscript type:	Regular Article
Date Submitted by the Author:	20-Sep-2012
Complete List of Authors:	Ebrahim, Weaam; Institut für Pharmazeutische Biologie und Biotechnologie, Heinrich-Heine-Universität Düsseldorf Aly, Amal; Institut für Pharmazeutische Biologie und Biotechnologie, Heinrich-Heine-Universität Düsseldorf Mándi, Attila; University of Debrecen, Organic Chemistry Wray, Victor; Helmholtz Centre for Infection Research, Essassi, El Mokhtar; Université Mohammed-V Agdal, Faculté des Sciences Ouchbani, Tarik; Université Mohammed-V Agdal, Faculté des Sciences Bouhfid, Rachid; Moroccan Foundation Advanced Science, Innovation and Research (MFAScIR), Institute of Nanomaterials and Nanotechnology (INANOTECH) Lin, Wenhan; Peking University, National Research Laboratories of Natural and Biomimetic Drugs Proksch, Peter; Institut für Pharmazeutische Biologie und Biotechnologie, Heinrich-Heine-Universität Düsseldorf Kurtan, Tibor; University of Debrecen, Organic Chemistry Debbab, Abdessamad; Institut für Pharmazeutische Biologie und Biotechnologie, Heinrich-Heine-Universität Düsseldorf
Keywords:	Cladanthus , endophytes, Embellisia, Structure elucidation, TDDFT ECD calculation

New Polyketides from *Embellisia eureka*, an endophyte of *Cladanthus arabicus*

WEAAM EBRAHIM,[1,5] AMAL H. ALY,[1] ATTILA MÁNDI,[3] VICTOR WRAY,[2] EL MOKHTAR ESSASSI,[6,7] TARIK OUCHBANI,[1,6] RACHID BOUHFID,[7] WENHAN LIN,[4] PETER PROKSCH,[1] TIBOR KURTÁN,[3] AND ABDESSAMAD DEBBAB[1]*

[1] Institut für Pharmazeutische Biologie und Biotechnologie, Heinrich-Heine-Universität Düsseldorf, Universitätsstrasse 1, Geb. 26.23, 40225 Düsseldorf, Germany.

[2] Helmholtz Centre for Infection Research, Inhoffenstraße 7, D-38124 Braunschweig, Germany.

[3] Department of Organic Chemistry, University of Debrecen, POB 20, 4010 Debrecen, Hungary.

[4] National Research Laboratories of Natural and Biomimetic Drugs, Peking University, Health Science Center, 100083 Beijing, People's Republic of China.

[5] Department of Pharmacognosy, Faculty of Pharmacy, Mansoura University, 35516 Mansoura, Egypt.

[6] Laboratoire de Chimie Organique Hétérocyclique, Faculté des Sciences, Université Mohammed-V Agdal, Avenue Ibn Batouta, BP. 1014, Rabat, Morocco.

[7] Moroccan Foundation Advanced Science, Innovation and Research (MFAScIR), Institute of Nanomaterials and Nanotechnology (INANOTECH), ENSET, Av. de l'Armée Royale, Madinat El Irfane 10100 - Rabat, Morocco.

* Corresponding author.

abdessamad.debbab@uni-duesseldorf.de Tel.: +49 211 81 15979; fax: +49 211 81 11923.

ABSTRACT Four new polyketides (**1**-**4**) were isolated from the EtOAc extract of the fungus *Embellisia eureka*, an endophyte of the Moroccan plant *Cladanthus arabicus* (Asteraceae). The structures of these new compounds were determined on the basis of one- and two-dimensional NMR spectroscopy as well as by high-resolution mass spectrometry. The absolute configurations of **1**-**3** were determined by TDDFT ECD calculations of solution conformers, online HPLC-ECD analysis and modified Mosher's method.

*KEY WORDS***:** *Cladanthus*, endophytes, *Embellisia*, Structure elucidation, TDDFT ECD calculation.

INTRODUCTION

Natural products from endophytic fungi continue to be an interesting research topic which attracts chemists and pharmacologists alike due to their unique skeletons and their important biological activities.[1-5] Several studies proved the role of such metabolites in mutualistic interactions between endophytes and host plants which in many cases result in benefits for both partners.[6] Recent reviews showed that endophytes are an inexhaustible source of bioactive secondary metabolites and lead structures, from which a significant number of natural drugs may be developed. These secondary metabolites include alkaloids, benzopyranones, chinones, flavonoids, phenolic acids, quinones, steroids, terpenoids, tetralones, xanthones and others.[2-5,7] Such bioactive metabolites find wide-ranging application as agrochemicals, antibiotics, immunosuppressants, antiparasitics, antioxidants and anticancer agents.[2-5,7-8] During our ongoing search for new bioactive metabolites from terrestrial endophytes,[9-12] we isolated an endophytic *Embellisia eureka* strain from stem tissues of the plant *Cladanthus arabicus* (Asteraceae) growing in Morocco. Literature survey on members of the genus *Embellisia* showed that a heptatrienoic acid-substituted bicyclic ketone derivative[13] and terpestacin[14] were previously reported from *Embellisia chlamydospora*. Moreover, hydroxyl substituted indolizidine alkaloids were obtained from *Embellisia oxytropis*.[15] Thus the fungal strain *E. eureka* evoked our attention since apparently it had only received scant attention in the past.

MATERIAL AND METHODS

General Experimental Procedures

Optical rotations were measured on a Perkin-Elmer-241 MC polarimeter. 1D and 2D NMR spectra were recorded on Bruker 300, ARX 400 or AVANCE DMX 600 NMR spectrometers. ESIMS and HRESIMS were obtained on Finnigan LCQ Deca and Micromass Qtof 2 mass spectrometers, respectively. ECD spectra were recorded on a J-810 spectropolarimeter.

Solvents were distilled prior to use, and spectral grade solvents were used for spectroscopic measurements. HPLC/ECD analysis: HPLC separations were carried out with a Jasco HPLC system on a Chiralpak IC column (5 µm, 150×4.6 mm) using hexane/isopropanol 6:4 as eluent. The HPLC/ECD and HPLC/UV traces were recorded at 270 nm with a Jasco J-810 CD spectropolarimeter equipped with a 1 cm pathlength HPLC flow cell and the chromatogram was zeroed right after the start of recording, and hence relative absorbance was measured. The on-line CD and UV spectra (200–400 nm) were recorded simultaneously at the maxima of the UV peaks where the flow was stopped. ECD ellipticity values were not corrected for concentration. For an HPLC-ECD spectrum, three consecutive scans were recorded and averaged with 2 nm bandwidth, 1 s response, and standard sensitivity. The HPLC-ECD spectrum of the eluent recorded in the same way was used as back-ground. The UV-absorption trace was recorded as high tension voltage (HTV) and converted to absorbance. The concentration of the injected sample was set so that the HT value did not exceed 500 V in the HT channel down to 220 nm.

Fungal Material

Fresh, healthy stems of *Cladanthus arabicus* (Asteraceae) were collected in September 2010 in Morocco. Stems were rinsed twice with sterilized distilled water. Surface sterilization was achieved by immersing the leaves in 70% ethanol for 2 min (twice) followed by rinsing twice in sterilized distilled water. The stems were then cleaved aseptically into small segments (approx.1 cm in length). The material was placed on a Petri dish (malt agar medium) containing chloramphenicol to suppress bacterial growth (medium composition: 15 g/L malt extract, 15 g/L agar, and 0.2 g/L chloramphenicol in distilled water, pH 7.4-7.8) and incubated at room temperature (22 °C). After several days, hyphae growing from the plant material were transferred to fresh plates with the same medium, incubated again for 10 days, and periodically checked for culture purity.

Identification of Fungal Cultures

Fungal cultures were identified according to a molecular biological protocol by DNA amplification and sequencing of the ITS region as described previously.[16] The sequence data have been submitted to GenBank, accession number HE653395. The fungal strain was identified as *Embellisia eureka*. A voucher strain (strain designation CATS2) is kept in the Institute of Pharmaceutical Biology and Biotechnology, Duesseldorf, Germany.

Cultivation

Twenty Erlenmeyer flasks (1L each) containing 100 g of rice and 100 mL of distilled water were autoclaved. A small part of the medium from a Petri dish containing the purified fungus was transferred under sterile conditions to the rice medium. The fungal strain was grown on solid rice medium at room temperature (22 °C) for 40 days.

Extraction and Fractionation

The culture was extracted with EtOAc. The EtOAc extract was washed with water, taken to dryness and partitioned between *n*-hexane and 90% MeOH. The 90% MeOH fraction was chromatographed over silica gel F_{254} (Merck, Darmstadt, Germany) using gradient elution (*n*-Hexane: EtOAC: DCM: MeOH). One of the resulting fractions (70 % EtOAc/30 % *n*-hexane) was subjected to Sephadex LH-20 using 100% methanol as mobile phase. Yields of compounds were as follows: **1/2** 2.5 mg, **3** 4 mg and **4** 1.5 mg.

rac-**Embeurekols**: yellow amorphous mass; $[\alpha]_D^{20}$ 0 (*c* 0.05, MeOH); ^1H and ^{13}C in DMSO-d_6, see table 1; HRESIMS *m/z* 241.0707 $[M+H]^+$ (calcd for $C_{11}H_{12}O_6$, 241.0707).

Embeurekol A: (*R*)-**1**: retention time (t_r) 4.48 min ; ECD data recorded online in hexane/isopropanol 6:4 as λ_{max} ($\Delta\varepsilon$): 323 (0.20), 271 (–2.46), 241 (–0.89), 225 (1.27), 217sh (1.23), negative below 210 nm.

Embeurekol B: (*S*)-**2**: retention time (t_r) 4.25 min (Chiralpak IC, 5 µm, 150×4.6 mm, hexane/isopropanol 6:4 eluent); ECD data recorded online in hexane/isopropanol 6:4 as λ_{max} ($\Delta\varepsilon$): 319 (–0.10), 271 (2.39), 240 (1.26), 226 (–1.50), 214sh (–1.29), positive below 210 nm.

Embeurekol C (3): yellow amorphous mass; $[\alpha]_D^{20}$ –17 (*c* 0.05, MeOH); ECD (CH_3CN, *c* = 3.8×10^{-4}) λ_{max} ($\Delta\varepsilon$): 301 (–0.71), 254 (3.27), 225 (2.06), 208 (–11.04). ^{1}H and ^{13}C in DMSO-d_6, see table 2; HRESIMS *m*/*z* 241.0688 $[M+H]^+$ (calcd for $C_{11}H_{12}O_6$, 241.0707).

Embeurekol D (4): yellow amorphous mass; $[\alpha]_D^{20}$ –8 (*c* 0.05, MeOH); ^{1}H and ^{13}C in DMSO-d_6, see table 2; HRESIMS *m*/*z* 285.0423 $[M+H]^+$ (calcd for $C_{12}H_{12}O_6S$, 285.0433).

Mosher Method

The reaction was performed according to a convenient Mosher ester procedure.[17]

Computational Section

Conformational searches were carried out by means of the Macromodel 9.7.211[18] software using Merck Molecular Force Field (MMFF) with implicit solvent model for chloroform. Geometry reoptimizations at B3LYP/6-31G(d) in vacuo and B3LYP/TZVP levels of theory applying a PCM solvent model for MeCN followed by TDDFT ECD calculations using various functionals (B3LYP, BH&HLYP, PBE0) and TZVP basis set were performed by the Gaussian 09[19] package. Boltzmann distributions were estimated from the ZPVE corrected B3LYP/6-31G(d) energies in the gas-phase calculations, and from the B3LYP/TZVP energies

in the PCM calculations. ECD spectra were generated as the sum of Gaussians[20] with 2400 cm^{-1} half-height width (corresponding to ca. 14 at 240 nm), using dipole-velocity computed rotational strengths for conformers above 3%. The MOLEKEL[21] software package was used for visualization of the results.

RESULTS AND DISCUSSION

The crude ethyl acetate extract of *Embellisia eureka*, cultured on solid rice medium, was taken to dryness and then partitioned between *n*-hexane and 90% methanol. The 90% methanol fraction was chromatographed over different stationary phases. Final purification by semi-preparative reversed-phase HPLC afforded four new compounds whose structures were elucidated by high resolution ESI mass spectrometry and NMR spectroscopy. These new compounds were identified as the polyketides named, embeurekols A (**1**) and B (**2**), embeurekol C (**3**) and embeurekol D (**4**).

Embeurekols A (**1**) and B (**2**) were obtained as a racemic mixture forming a yellowish amorphous mass. The HRESI-MS exhibited a strong peak at *m/z* 241.0707 $[M+H]^+$ indicating a molecular formula of $C_{11}H_{12}O_6$ (calcd for 241.0707) for both **1** and **2**. The NMR data of **1** and **2** showed only one set of signals. Comparison of NMR data of embeurekols **1** and **2** with those of the known 3,6,8-trihydroxy-3-methyl-3,4-dihydroisocoumarin, isolated from *Alternaria kikuchiana* by Kameda *et al.*,[22] showed a close relationship except for an extra methoxy group in embeurekols. The ^1H NMR spectrum showed a singlet at δ_H 1.62 ppm assigned for CH_3-11, two doublets at δ_H 3.10 (d, 16.9 Hz) and 3.18 ppm (d, 16.9 Hz) integrated for 2 protons, attributed to the CH_2-4 geminal protons, an aromatic singlet at δ_H 6.29 ppm assigned to H-7, a singlet integrated for 3 protons at δ_H 3.63 ppm assigned to OCH_3-12, and three singlets at δ_H 7.42, δ_H 10.70 and 10.90 ppm which were attributed to the hydroxyl groups 3-OH, 6-OH and 8-OH, respectively. In the HMBC spectrum, H-7 showed strong ^3J correlations to C-5 and C-9, ^2J

correlations to C-6 and C-8 and a weak ^{4}Jcorrelation to the *keto*-group C-1. Further inspection of the HMBC spectrum revealed correlations of CH_3-11 at δ_H 1.62 ppm to C-3 (δ_C 105.1) and C-4 (δ_C 32.2), and of CH_2-4 at δ_H 3.10 and 3.18 ppm to C-3, C-5, C-9, C-10 (δ_C 130.9) and C-11 (δ_C 22.3). The attachment of the methoxy group to the aromatic ring was confirmed by its HMBC correlation to C-5. The structure was further confirmed by a ROESY experiment. The OCH_3-12 signal at δ_H 3.63 ppm showed strong ROESY correlations to CH_2-4 at δ_H 3.10 and 3.18 ppm, whereas H-7 at δ_H 6.29 ppm showed strong ROESY correlations to both aromatic hydroxyl groups at δ_H 10.70 and 10.90 ppm indicating its position between both hydroxyls.

The ECD measurement of embeurekols A (**1**) and B (**2**) did not afford a distinct ECD spectrum indicating that either it is a racemic mixture or it has two equilibrating conformers with axial or equatorial 3-OH of comparable populations. Thus a chiral HPLC analysis was performed, which could confirm that the sample is a racemic mixture and the two enantiomers were base-line separated on a Chiralpak IC column and identified by HPLC/UV and HPLC/ECD chromatograms. Since online HPLC-ECD measurements had been found an efficient tool to study stereoisomeric mixtures of natural products,[23,24] the online HPLC-ECD spectra of the separated enantiomers were recorded showing characteristic transitions of dihydroisocoumarins with mirror image relationship. The second-eluted enantiomer had a weak positive CE at 323 nm ($^{1}L_b$ type), two negative transitions at 271 and 241 nm (n–π* and π–π*), a positive one at 225 nm (π–π*) and the ECD curve had negative values below 210 nm. The heteroring of dihydroisocoumarins adopts a half-chair or envelop conformation, the helicity of which is defined by the $\omega_{C\text{-}5a,C\text{-}4,C\text{-}3,O}$ torsional angle. Negative $\omega_{C\text{-}5a,C\text{-}4,C\text{-}3,O}$ torsional angle implies *M* helicity of the heteroring, which results in negative n–π* CE regardless of the substitution pattern of the aromatic ring. This helicity rule was established on the basis of synthetic 3-substituted dihydroisocoumarin derivatives[25] and it was confirmed by TDDFT ECD calculations and applied to the configurational assignment of natural dihydroisocoumarins.[26-28] According to this helicity rule, the negative n–π* CE of the second-eluted enantiomer at 271 nm

derives from *M* helicity of the heteroring. For the configurational assignment, one has to know whether the 3-OH or 3-Me group adopts equatorial orientation in the low-energy conformers. Thus a conformational analysis was carried out; the initial MMFF conformers were reoptimized by both B3LYP/6-31G(d) in vacuo and B3LYP/TZVP applying a PCM solvent model for MeCN. The two methods came to the same conclusion; the 3-OH preferably adopts *axial* orientation. In the B3LYP/TZVP optimization, 82.7% population was represented by the 3-OH_{ax} and 10.5% by the 3-OH_{eq} conformers when populations above 3% were considered (Figure 1). The preferred 3-OH_{ax} conformation also corroborates the observed ROE effects among the equatorial 3-Me and both 4-Hs. The *M* helicity of the heteroring and the *axial* orientation of 3-OH defines the (3*R*) absolute configuration of the second-eluted enantiomer, which was named embeurekol A (**1**). Since the n–π* CE of dihydroisocoumarins often overlaps with π–π* transitions, our assignment was also confirmed by the TDDFT ECD calculation of the solution conformers using various functionals (B3LYP, BH&HLYP, PBE0) and TZVP basis set. The Boltzmann-averaged ECD curve of (*R*)-**1** reproduced well the experimental curve of the second-eluted enantiomer, which unambiguously confirmed our former assignment by the semi-empirical ECD rule (Figure 2). Thus compounds **1** and **2** were found to be new enantiomeric natural products for which the names embeurekol A and B are assigned, respectively.

Embeurekol C (**3**) was isolated as yellowish amorphous mass. The HRESI-MS exhibited a strong peak at *m*/*z* 241.0688 $[M+H]^+$ indicating the molecular formula $C_{11}H_{12}O_6$ (calcd for 241.0707). Comparison of NMR data of **3** with those of the known acetophthalidin, previously isolated from *Aspergillus fumigates*,[29] showed a close relationship except for an extra methoxy group as well as reduction of the C-1′ ketone carbonyl of acetophthalidin in **3**. ^{1}H NMR spectrum showed a doublet resonating at δ_H 0.73 ppm (J=6.3 Hz) assigned for CH_3-2′, a multiplet at δ_H 4.24 ppm for H-1′, a doublet at δ_H 5.45 ppm (J=2.3 Hz) for H-3, a singlet at δ_H

3.69 ppm for OCH_3-10, an aromatic singlet at δ_H 6.45 ppm for H-6 and two singlets at δ_H 10.21 and 10.46 ppm assigned for the aromatic hydroxyl groups 7-OH and 5-OH, respectively. The ^{1}H-^{1}H COSY spectrum showed one distinct spin system including CH_3(2′)CH(1′)OH(1′)CH(3). In the HMBC spectrum, H-6 showed strong ^3J correlations to C-4 and C-8, whereas ^2J correlations to C-5 and C-7 and a weak ^4J correlation to the C-1 carbonyl group were likewise observed. Moreover, correlations of CH_3-2′ at δ_H 0.73 ppm to C-1′ and C-3, of H-1′ at δ_H 4.24 ppm to C-2′ and C-3 and of H-3 at δ_H 5.45 ppm to C-1, C-4, C-8, C-9, C-1′ and C-2′ as well as to C-5 and C-7 *via* ^4J-correlation, were also detected. The attachment of the methoxy group (δ_H 3.69 ppm) to the aromatic ring at position C-4 was confirmed by its HMBC correlation to C-4. The structure was further confirmed by a ROESY experiment. The OCH_3-10 at δ_H 3.69 ppm showed strong ROESY correlations to H-1′ at δ_H 4.24 ppm, H-3 at δ_H 5.45 ppm, and CH_3-2′ at δ_H 0.73 ppm. In addition, H-6 resonating at δ_H 6.45 ppm showed a strong ROESY correlation to both aromatic hydroxyl groups at δ_H 10.21 and 10.46 ppm indicating its position between both hydroxyls.

Embeurekol C (**3**) was optically active and it showed negative CEs at 301 (n–π*) and 208 nm and positive ones at 254 and 225 nm. Since the ECD spectrum is governed by the absolute configuration of the fused heteroring, ECD calculation could be used to determine the absolute configuration of C-3. The B3LYP/TZVP reoptimization (PCM solvent model for MeCN) of the initial MMFF conformers of (3*S*,1′*S*)-**3** afforded five conformers above 3% population totalling 90.8%. Two major conformations could be identified; in the low-energy one represented by two conformers (54.3% and 8.3%), 3-H is *anti-periplanar* with 1′-H and 1′-OH is hydrogen-bonded to 4-OMe, while in the higher-energy one manifested in three conformers (18.4%, 5.0% and 4.8%), the 3-H is *anti-periplanar* with the C-2′ (Figure 4). The Boltzmann-averaged TDDFT ECD spectra of (3*S*,1′*S*)-**3** was in agreement with the experimental curve (Figure 5) allowing the configurational assignment of C-3 as (*S*). Moreover, the B3LYP/TZVP optimization (Figure 6) and ECD calculations of the

diastereomeric (3*R*,1′*S*)-**3** conformers were also achieved, which resulted in a mirror image ECD curve of the experimental spectrum confirming the above assignment. It is worth noting that ECD spectra of the related phthalide metabolites (+)-spirolaxine and sporotricale could not be used for the configurational assignment of C-3, since they showed markedly different ECD curves, which can be attributed to the chelating 7-OH group of **3**.[30]

Since the relative configuration of C-1′ could not be unambiguously determined, the modified Mosher method was applied[17] to deduce the absolute configuration at C-1′. The chemical shift differences between the (*S*)- and the (*R*)-MTPA esters allowed the assignment of the absolute configuration as (1′S) (Table 3). Thus compound **3** was identified as a new natural product with (−)-(3*S*,1′*S*) absolute configuration and named as embeurekol C.

Embeurekol D (**4**) was isolated as yellowish amorphous mass. The HRESI-MS exhibited a strong peak at *m/z* 285.0423 $[M+H]^+$ indicating the molecular formula $C_{12}H_{12}O_6S$ (calcd for 285.0433). NMR data of **4** were very similar to those of **3**. ^{1}H NMR spectrum showed a singlet at δ_H 2.13 ppm for CH_3-2′, a singlet at δ_H 1.80 ppm for CH_3-3′, a singlet at δ_H 3.69 ppm for OCH_3-10, an aromatic singlet at δ_H 6.61 ppm for H-6, and two singlets at δ_H 10.81 and 11.00 ppm attributed to the aromatic hydroxyl groups 7-OH and 5-OH, respectively. The ^{13}C chemical shift of CH_3-3′ (δ_C 11.2 ppm) indicated its attachment to a sulfur atom (which is also confirmed by HRMS). The attachment of SCH_3-3′ to C-3 was confirmed by the HMBC correlation of CH_3-3′ to C-3. In the HMBC spectrum, H-6 showed strong ^3J correlations to C-4 and C-8, ^2J correlations to C-5 and C-7, and a weak ^4J correlation to the *keto*-group C-1. Further inspection of the HMBC spectrum revealed additional correlations of CH_3-2′ at δ_H 2.13 ppm to C-1′ and C-3. The attachment of the aromatic methoxy group (δ_H 3.69 ppm) was confirmed by its ^3J correlation to C-4. The structure was further confirmed by a ROESY experiment. H-6 at δ_H 6.61 ppm showed strong correlations to both aromatic hydroxyl groups at δ_H 10.81 and 11.00 ppm indicating its position between both hydroxyl groups. Unfortunately, **4** decomposed before the

ECD measurement and thus its absolute configuration could not be determined. According to its spectroscopic data, compound **4** is a new natural product which is named embeurekol D.

Compounds **1/2** and **3** were evaluated for their biological activities, including cytotoxic activity against murine L5178Y cells and antibacterial activity against multi drug resistant strains of *Staphylococcus aureus*, *Streptococcus pneumoniae*, *Enterococcus faecium* and *Enterococcus cloacae*. In addition, anti-fungal activity of the isolated compounds against drug resistant strains of *Aspergillus fumigatus*, *Aspergillus faecalis*, *Candida albicans* and *Candida krusei* was likewise investigated. However, none of the isolated natural products proved to be active in the bioassays carried out.

Conclusion

Four new polyketides (**1**-**4**) were isolated and identified from the endophytic fungus *Embellisia eureka*, an endophyte of *Cladanthus arabicus*. Absolute configurations of the isolated structures (**1**-**3**) were determined by TDDFT ECD calculations of their solution conformers. In addition, the modified Mosher method was applied to determine the absolute configuration at C-1′ in **3**, which could not be unambiguously determined by CD. However, **1**-**3** were inactive when tested for their antimicrobial and cytotoxic activities.

Acknowledgements

This project was supported by grants of the BMBF (to P.P. and A.D.) and MOST to W.L. A scholarship (Grant No. 10/6/117) granted and financed by the Egyptian Government (Ministry of High Education) to W.E. is gratefully acknowledged. T.K. and A.M. thank the HURO/0901/274/2.2.2 project (websites: www.huro-cbc.eu and www.hungary-romania-cbc.eu) and the National Information Infrastructure Development Institute (NIIFI 10038).

References

1. Li J, Zhao GZ, Chen HH, Wang HB, Qin S, Zhu WY, Xu LL, Jiang CL, Li WJ. Antitumour and antimicrobial activities of endophytic streptomycetes from pharmaceutical plants in rainforest. Lett Appl Microbiol. 2008;47:574-580.
2. Aly AH, Debbab A, Kjer J, Proksch P. Fungal endophytes from higher plant: a prolific source of phytochemicals and other bioactive natural products. Fungal Divers 2010;41:1-16.
3. Aly AH, Debbab A, Proksch P. Fungal endophytes: Unique plant inhabitants with great promises. Appl Microbiol Biot 2011;90:1829-1845.
4. Debbab A, Aly AH, Proksch P. Bioactive secondary metabolites from endophytes and associated marine derived fungi. Fungal Divers 2011;49:1-12.
5. Debbab A, Aly AH, Proksch P. Endophytes and associated marine derived fungi-ecological and chemical perspectives. Fungal Divers 2012; DOI 10.1007/s13225-012-0191-8.
6. Kogel KH, Franken P, Huckelhoven R. Endophyte or parasite-what decides?. Curr. Opinion plant physiol 2006;9:358-363.
7. Tan RX, Zou WX. Endophytes: a rich source of functional metabolites. Nat Prod Rep 2001;18:448-459.
8. Gunatilaka AAL. Natural Products from Plant-Associated Microorganisms: Distribution, Structural Diversity, Bioactivity, and Implications of Their Occurrence. J Nat Prod 2006;69:509-526.
9. Aly AH, Debbab A, Clements C, Edrada-Ebel R, Orlikova B, Diederich M, Wray V, Lin WH, Proksch P. NF kappa B inhibitors and antitrypanosomal metabolites from endophytic fungus *Penicillium* sp. isolated from *Limonium tubiflorum*. Bioorg Med Chem 2011;19:414-421.
10. Ebrahim W, Aly AH, Mándi A, Totzke F, Kubbutat MH, Wray V, Lin WH, Dai H, Proksch P, Kurtán T, Debbab A. Decalactone derivatives from *Corynespora cassiicola*, an endophytic fungus of the mangrove plant *Laguncularia racemosa*. Eur J Org Chem 2012;3476–3484.
11. Debbab A, Aly AH, Edrada-Ebel R, Wray V, Muller WE, Totzke F, Zirrgiebel U, Schachtele C, Kubbutat MH, Lin WH, Mosaddak M, Hakiki A, Proksch P, Ebel R. Bioactive metabolites from the endophytic fungus *Stemphylium globuliferum* isolated from *Mentha pulegium*. J Nat Prod 2009;72:626-631.

12. Debbab A, Aly AH, Edrada-Ebel R, Wray V, Pretsch P, Pescitelli G, Kurtan T, Proksch P. New anthracene derivatives – Structure elucidation and antimicrobial activity. Eur J Org Chem 2012;1351-1359.
13. Kwon HJ, Jung H, Shin JH, Kim CJ, Rho J, Lee H, Int. Appl. 2005, WO 2005003076 A1 20050113.
14. Jung HJ, Lee HB, Kim CJ, Rho JR, Shin JH, Kwon HJ. Anti-angiogenic activity of terpestacin, a bicyclo sesterterpene from *Embellisia chlamydospora*. J Antibiot 2003;56:492-496.
15. Shi D, Li L, Zheng M, Li G, Zhang H, Wang Q. Preliminary study on the isolation and purification of active secondary metabolites in the fermentation broth of *Embellisia oxytropis*. Anhui Nongye Kexue 2009;37:16213-16215.
16. Wang S, Li XM, Teuscher F, Li DL, Diesel A, Ebel R, Proksch P, Wang BG. Chaetopyranin, a benzaldehyde derivative, and other related metabolites from *Chaetomium globosum*, an endophytic fungus derived from the marine red alga *Polysiphonia urceolata*. J Nat Prod 2006;69:1622-1625.
17. Su BN, Park EJ, Mbwambo ZH, Santarsiero BD, Mesecar AD, Fong HHS, Pezzuto JM, Kinghorn AD. New chemical constituents of *Euphorbia quinquecostata* and absolute configuration assignment by a convenient Mosher ester procedure carried out in NMR tubes. J Nat Prod 2002;65:1278–1282.
18. MacroModel, Schrödinger LLC, 2009. http://www.schrodinger.com/Products/macromodel.html.
19. Frisch MJ, Trucks GW, Schlegel HB, Scuseria GE, Robb MA, Cheeseman JR, Scalmani G, Barone V, Mennucci B, Petersson GA, Nakatsuji H, Caricato M, Li X, Hratchian HP, Izmaylov AF, Bloino J, Zheng G, Sonnenberg JL, Hada M, Ehara M, Toyota K, Fukuda R, Hasegawa J, Ishida M, Nakajima T, Honda Y, Kitao O, Nakai H, Vreven T, Montgomery JA, Peralta JEJr, Ogliaro F, Bearpark M, Heyd JJ, Brothers E, Kudin KN, Staroverov VN, Kobayashi R, Normand J, Raghavachari K, Rendell A, Burant JC, Iyengar SS, Tomasi J, Cossi M, Rega N, Millam JM, Klene M, Knox JE, Cross JB, Bakken V, Adamo C, Jaramillo J, Gomperts R, Stratmann RE, Yazyev O, Austin AJ, Cammi R, Pomelli C, Ochterski JM, Martin RL, Morokuma K, Zakrzewski VG, Voth GA, Salvador P, Dannenberg JJ, Dapprich S, Daniels AD, Farkas O, Foresman JB, Ortiz JV, Cioslowski J, Fox DJ, Gaussian 09, Revision B.01, 2010, Gaussian, Inc., Wallingford CT.

20. Stephens PJ, Harada N. ECD cotton effect approximated by the Gaussian curve and other methods. Chirality 2010;22:229-233.
21. U. Varetto, MOLEKEL 5.4., 2009, Swiss National Supercomputing Centre: Manno, Switzerland.
22. Kameda K, Aoki H, Tanaka H, Namiki M. Metabolites of *Alternaria kikuchiana*, a phytopathogenic fungus of Japanese pear. Agric Biol Chem 1973;37:2137-2146.
23. Dai J, Krohn K, Flörke U, Draeger S, Schulz B, Kiss-Szikszai A, Antus S, Kurtán T, van Ree T. Metabolites from the endophytic fungus *Nodulisporium* sp. from *Juniperus ce*. Eur J Org Chem 2006;3498-3506.
24. Yao S, Tang C-P, Ye Y, Kurtán T, Kiss-Szikszai A, Antus S, Pescitelli G, Salvadori P, Krohn K. Stereochemistry of atropisomeric 9,10-dihydrophenanthrene dimers from *Pholidota chinensis*. Tetrahedron: Asymmetry 2008;19:2007-2014.
25. Kerti G, Kurtán T, Illyés T-Z, Kövér KE, Sólyom S, Pescitelli G, Fujioka N, Berova N, Antus S. Enantioselective synthesis of 3-methylisochromans and determination of their absolute configurations by circular dichroism. Eur J Org Chem 2007;296-305.
26. Krohn K, Kock I, Elsässer B, Flörke U, Schulz B, Draeger S, Pescitelli G, Antus S, Kurtán T. New natural products from the endophytic fungus *Ascochyta* sp. from *Meliotus dentatus*. Eur J Org Chem 2007;1123-1129.
27. Hussain H, Akhtar N, Draeger S, Schulz B, Pescitelli G, Salvadori P, Antus S, Kurtán T, Krohn K. New bioactive 2,3-epoxycyclohexenes and isocoumarins from the endophytic fungus *Phomopsis* sp. from *Laurus Azorica*. Eur J Org Chem 2009;749-756.
28. Kurtán T, Antus S, Pescitelli G, Electronic CD of Benzene and other Aromatic Chromophores for Determination of Absolute Configuration, in Comprehensive Chiroptical Spectroscopy: Applications in Stereochemical Analysis of Synthetic Compounds, Natural Products, and Biomolecules, Volume 2 (eds N. Berova, P. L. Polavarapu, K. Nakanishi and R. W. Woody), John Wiley & Sons, Inc., Hoboken, NJ, USA., 2012, vol 2, pp 73-114.
29. Cui CB, Ubukata M, Kakeya H, Onose R, Okada G, Takahashi I, Isono K, Osada H. Acetophthalidin, a novel inhibitor of mammalian cell cycle, produced by a fungus isolated from a sea sediment. J Antibiot 1996;49:216-219.
30. Bava A, Dallavalle S, Fronza G, Nasini G, de Pava OV. Absolute configuration of sporotricale and structure of 6-hydroxysporotricale. J Nat Prod 2006;69:1793-1795.

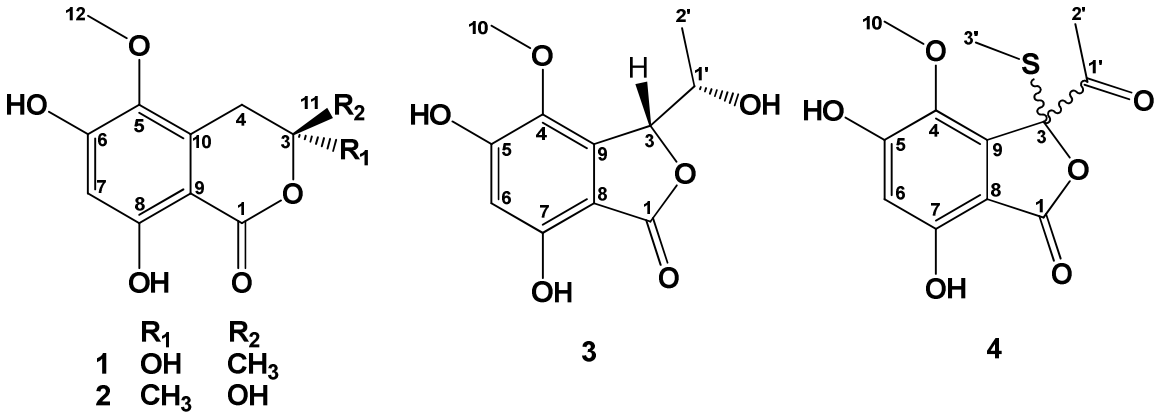

Chart 1. Structures of isolated compounds

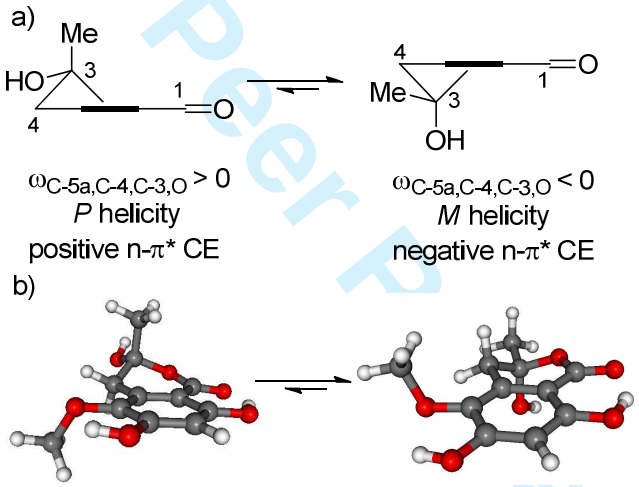

Figure 1. Equilibrating *P* and *M* helicity envelop conformers and helicity rule of (*R*)-**1** (second-eluted enantiomer) as viewed from the direction of the benzene ring (a) and as lowest-energy *P* and *M* helicity B3LYP/TZVP conformers (b).

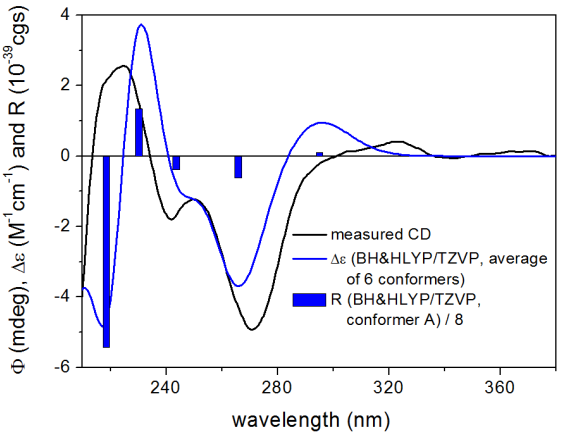

Figure 2. Online HPLC-ECD spectrum of (*R*)-**1** (second-eluted enantiomer) in hexane/isopropanol 6:4 compared with the Boltzman-weighted PBE0/TZVP spectrum calculated for six low-energy conformers of (*R*)-**1**. Bars represent rotational strengths of the lowest-energy conformers and online HPLC-ECD spectrum is scaled to the computed curve.

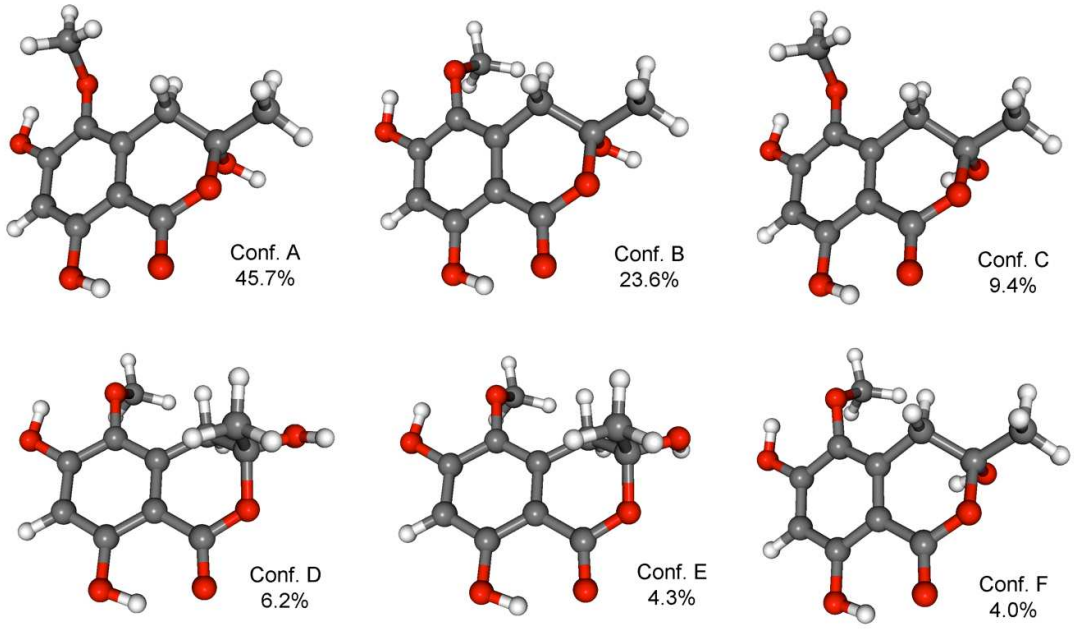

Figure 3. Solution conformers and populations (above 3%) of (*R*)-**1** obtained by B3LYP/TZVP reoptimization (PCM solvent model for acetonitrile) of MMFF conformers.

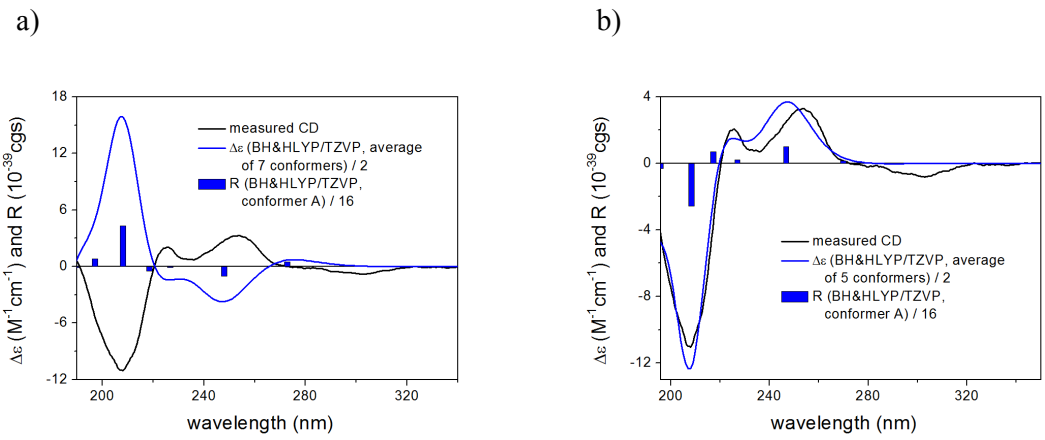

Figure 4. Experimental ECD spectrum of **3** in acetonitrile compared with the Boltzmann-weighted BH&HLYP/TZVP spectra calculated for the seven solution conformers of diastereomers (3*S*,1′*S*)-**3** (a) and (3*R*,1′*S*)-**3** (b).

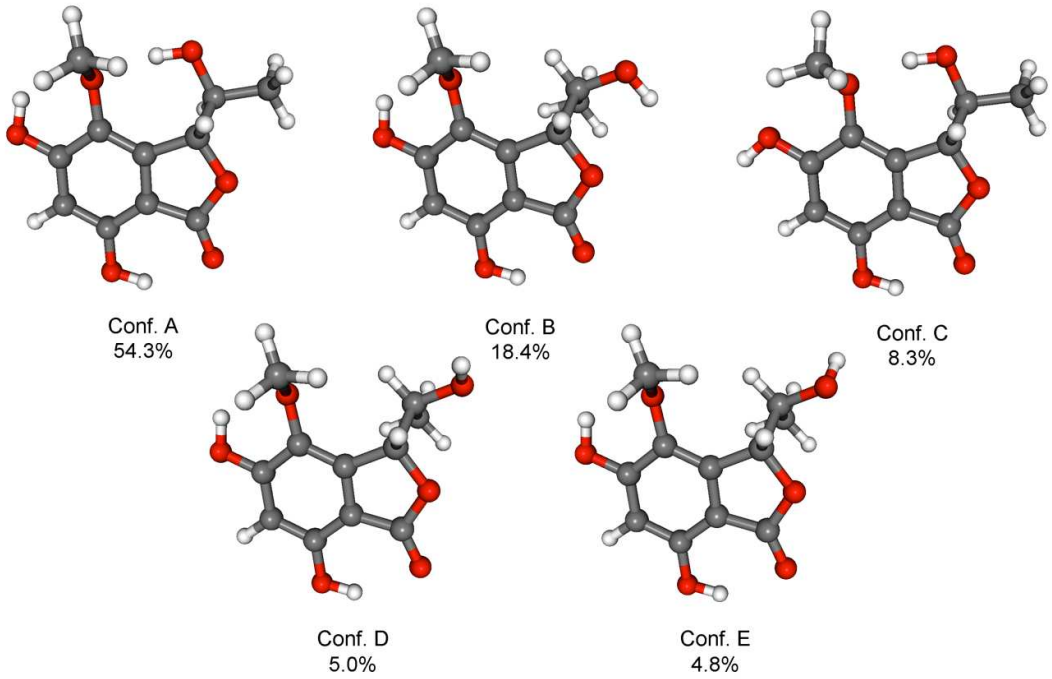

Figure 5. Solution conformers and populations (above 3%) of (3*S*,1′*S*)-**3** obtained by B3LYP/TZVP reoptimization (PCM solvent model for acetonitrile) of MMFF conformers.

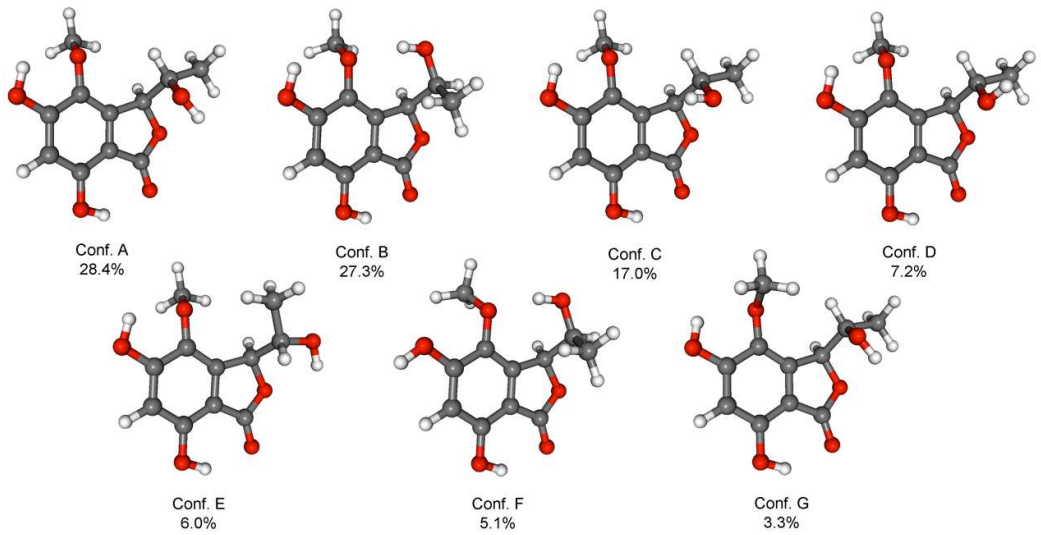

Figure 6. Solution conformers and populations (above 3%) of (3*R*,1′*S*)-**3** obtained by B3LYP/TZVP reoptimization (PCM solvent model for acetonitrile) of MMFF conformers.

Table 1: ^{1}H (600 MHz) and ^{13}C (150 MHz) NMR data (ppm) of compounds 1/2 (DMSO-d_6).

No.	1/2				
	δ_C	δ_H (multiplicity, coupling constant, integral)	COSY	HMBC(H→C)	ROESY
1	168.2 (C)				
3	105.1 (CH)				
4	32.2 (CH_2)	A 3.10 (d, J = 16.9 Hz, 1H)	4B	3, 5, 9, 10, 11	11, 12
		B 3.18 (d, J = 16.9 Hz, 1H)	4A	3, 7, 9, 10, 11	11, 12
5	137.8 (C)				
6	158.3 (C)				
7	101.6 (CH)	6.29 (s, 1H)		1, 5, 6, 8, 9	6-OH, 8-OH
8	159.1 (C)				
9	98.5 (C)				
10	130.9 (C)				
11	22.3 (CH_3)	1.62 (s, 3H)		3, 4	4A, 4B
12	60.2 (CH_3)	3.63 (s, 3H)		7	4A, 4B
3-OH		7.42, br. s			
6-OH		10.70, s		5, 6, 7	7
8-OH		10.90, s		7, 8, 9	7

Table 2: NMR data of embeurekol C (3) and embeurekol D (4).

No.	3*					4•			
	δ_C	δ_H	COSY	HMBC	ROESY	δ_C	δ_H	HMBC	ROESY
1	167.9 (C)					165.9 (C)			
2									
3	82.0 (CH)	5.45 (d, J = 2.3 Hz, 1H)	1′	1, 4,5, 7,8, 9, 1′, 2′	OCH_3-4, 2′	94.7 (C)			
4	134.2 (C)					135.3 (C)			
5	156.7 (C)					159.2 (C)			
6	104.4 (CH)	6.45(s, 1H)		1, 4, 5, 7, 8, 9	5-OH, 7-OH	106.6 (CH)	6.61 (s, 1H)	1, 4, 5, 7, 8	5-OH, 7-OH
7	153.6 (C)					154.5 (C)			
8	102.8 (C)					101.5 (C)			
9	140.4 (C)					137.6 (C)			
1′	66.1 (CH)	4.24 (m, 1H)	2′, 3	2′, 3		197.9 (C)			
2′	15.1 (CH_3)	0.73 (d, J = 6.3 Hz, 3H)	1′	1′, 3		24.9 (CH_3)	2,13 (s, 3H)	3, 1′	
3′						11.2 (CH_3)	1.80 (s, 3H)	3	
10	59.8 (CH_3)	3.69 (s, 3H)		4	3	60.6 (CH_3)	3.69 (s, 3H)	4	
5-OH		10.46, s		4, 5	6		11.00, s	4, 5, 6	6
7-OH		10.21, br. s			6		10.81, s	7, 8	6

*) Measured at 300 (^{1}H) and 75 (^{13}C) MHz (DMSO-d_6).

•) Measured at 400 (^{1}H) and 100 (^{13}C) MHz (DMSO-d_6).

Table 3: Chemical shift differences between the (*S*)-MTPA and (*R*)-MTPA esters of 3.

Proton no.	Chemical shift (δ_H, in C_5D_5N, at 500 MHz)			
	3	(*S*)-MTPA *ester*	(*R*)-MTPA *ester*	$\Delta\ \delta S - \delta R$
2□	1.03047	1.2948	1.2954	-0.0006
3	6.0673	6.0593	6.0583	+0.001
6	6.9355	7.0739	7.0547	+0.0192
OCH_3-5	3.9077	3.9083	3.9075	+0.0008